Research article

Silica-coated magnetic particles for efficient RNA extraction for SARS-CoV-2 detection

Natalia Capriotti [a,1], Leslie C. Amorós Morales [b,1], Elisa de Sousa [c], Luciana Juncal [c], Matias Luis Pidre [b], Lucila Traverso [a], Maria Florencia López [b], Maria Leticia Ferelli [b], Gabriel Lavorato [d], Cristian Lillo [d], Odin Vazquez Robaina [c], Nicolas Mele [c], Carolina Vericat [d], Patricia Schilardi [d], Alejandra Fabiana Cabrera [c], Silvana Stewart [c], Mariano H. Fonticelli [d], Pedro Mendoza Zéliz [c], Sheila Ons [a], Victor Romanowski [b], Claudia Rodríguez Torres [c,*]

[a] *Laboratorio de Neurobiología de Insectos (LNI), Centro Regional de Estudios Genómicos, Facultad de Ciencias Exactas, Universidad Nacional de La Plata, CENEXA, CONICET, La Plata, Buenos Aires, Argentina*
[b] *Instituto de Biotecnología y Biología Molecular (IBBM), Facultad de Ciencias Exactas, Universidad Nacional de La Plata-CONICET, La Plata, Argentina*
[c] *IFLP-CCT-La Plata-CONICET and Departamento de Física, Facultad de Ciencias Exactas, C. C. 67, Universidad Nacional de La Plata, 1900, La Plata, Argentina*
[d] *Instituto de Investigaciones Fisicoquímicas Teóricas y Aplicadas (INIFTA), Facultad de Ciencias Exactas, Universidad Nacional de La Plata - CONICET, 1900, La Plata, Buenos Aires, Argentina*

ARTICLE INFO

ABSTRACT

Molecular diagnostic methods to detect and quantify viral RNA in clinical samples rely on the purification of the genetic material prior to reverse transcription polymerase chain reaction (qRT-PCR). Due to the large number of samples processed in clinical laboratories, automation has become a necessity in order to increase method processivity and maximize throughput per unit of time. An attractive option for isolating viral RNA is based on the magnetic solid phase separation procedure (MSPS) using magnetic microparticles. This method offers the advantage over other alternative methods of making it possible to automate the process. In this study, we report the results of the MSPS method based on magnetic microparticles obtained by a simple synthesis process, to purify RNA from oro- and nasopharyngeal swab samples of patients suspected of COVID-19 provided by three diagnostic laboratories located in the Buenos Aires Province, Argentina. Magnetite nanoparticles of Fe_3O_4 (MNPs) were synthesized by the coprecipitation method and then coated with silica (SiO_2) produced by hydrolysis of tetraethyl orthosilicate (TEOS). After preliminary tests on samples from the A549 human lung cell line and swabs, an extraction protocol was developed. The quantity and purity of the RNA obtained were determined by gel electrophoresis, spectrophotometry, and qRT-PCR. Tests on samples from naso- and oropharyngeal swabs were performed in order to validate the method for RNA purification in high-throughput SARS-CoV-2 diagnosis by qRT-PCR. The method was compared to the spin columns method and the automated method using commercial magnetic particles. The results show that the method developed is efficient for RNA extraction from nasal and oropharyngeal

swab samples, and also comparable to other extraction methods in terms of sensitivity for SARS-CoV-2 detection. Of note, this procedure and reagents developed locally were intended to overcome the shortage of imported diagnostic supplies as the sudden spread of COVID-19 required unexpected quantities of nucleic acid isolation and diagnostic kits worldwide.

1. Introduction

Severe acute respiratory syndrome coronavirus 2 (SARS-CoV-2) is an enveloped RNA virus and the etiologic agent of Coronavirus disease 2019 (Covid-19), declared as a pandemic by the World Health Organization (WHO) on March 11th, 2020 [1]. Consequently, Argentina's government decreed a preventive lock-down on March 20th, 2020, in order to reduce the spread of the virus [2]. Despite efforts, more than 1,600,000 positive cases were reported by the end of 2020 in the country [3]. In this emergency context, the development of strategies for high-throughput SARS-CoV-2 diagnosis was crucial to deal with the pandemic situation, not only in Argentina but around the world.

Molecular diagnostics have been used to detect a wide variety of pathogenic viruses due to their high sensitivity and specificity [4, 5]. Many strategies based on antibody or antigen detection have been developed for Covid-19 diagnosis. However, real-time reverse transcription polymerase chain reaction (qRT-PCR) remains the validated assay for early diagnosis in patients with suspected SARS-CoV-2 infection. The qRT-PCR method is a reliable, standard and routinely used technique for the analysis and quantification of ribonucleic acids (RNA) from pathogens in laboratories and clinical diagnostics. It has been successfully applied for the detection of several viral pathogens (syndrome coronavirus, Middle East respiratory syndrome coronavirus, Zika, Dengue, Influenza A and others) [6,7]. qRT-PCR protocols for the detection of these viruses are widely standardized, optimized, and validated. A necessary requirement in qRT-PCR diagnosis is the purification of RNA from biological samples. This is achieved with the proper choice of a method that separates RNA from proteins, polysaccharides, and lipids. Currently, different commercial kits are recommended for this step but most of them implement laborious and expensive methods based on the use of silica membranes in columns, which need specific equipment such as a refrigerated centrifuge. The aim of this work was the development of a simpler strategy for RNA extraction for rapid SARS-CoV-2 detection that does not require centrifugation nor other sophisticated lab equipment and that can be automated.

An attractive option for the purification of viral RNA is based on the magnetic solid phase separation (MSPS) procedure using magnetic beads (MBs) [8,9]. MBs consist of a core of magnetic nanoparticles coated with an inorganic or polymeric organic material (silica, cellulose or polystyrene, etc.). The nanometer size of the particles results in a single domain structure with superparamagnetic behavior. This characteristic is fundamental for two reasons: it ensures a high magnetic response to small applied fields, while in the absence of field the MBs do not present a net magnetic moment due to thermal fluctuations [10]. After a lysis step, the MBs are added to the sample. In the presence of an appropriate salt concentration, binding of RNA to the charged surface of the MBs occurs. Subsequently, with the application of a magnetic field, the MBs are immobilized and separated along with the nucleic acids. After some washing steps, the purified nucleic acids are released from the MBs in the presence of water or a buffer with a low concentration of salts [11]. Separation, washing and elution of nucleic acids are achieved without centrifugation or filtration. The use of MBs in the isolation of nucleic acids offers, among many benefits, the advantage over other existing methods of making it possible to automate the whole process. Due to the large number of samples processed in laboratories nowadays, automation has become a necessity in order to increase processivity. Automated methods maximize the throughput in terms of samples/hour and minimize staff exposure to pathogens and toxic compounds.

Various methods for extracting nucleic acids using magnetic beads have been explored and many MBs-based extraction kits have become commercial products. These methods have been successfully tested for DNA and/or RNA purification from prokaryote and eukaryote cells [12], Zika virus [13] diagnosis, viral pathogens causing acute respiratory infections [14], and hepatocellular carcinoma [15], among others (see Ref. [8]). Furthermore, MBs-based methods have been proven to be suitable for SARS-CoV-2 RNA extraction, in which commercial magnetic beads or in-house manufactured carboxyl-coated magnetic beads are generally employed [16–19]. Here, we present a study of the application of the magnetic beads purification method (MB-UNLP) using silica-coated magnetic beads (MNPs@SiO$_2$) obtained by a simple synthesis protocol. We explored the efficiency of the MB-UNLP method in purifying RNA from cells in culture and from swab samples from patients with suspected COVID-19 from three diagnostic laboratories: Rossi Hospital, Public Health Laboratory, and Evita Hospital, which are located in the Buenos Aires Province, Argentina. Our results indicate that this method is robust for RNA purification in the diagnosis process.

2. Materials and methods

2.1. Chemicals and reagents

FeCl$_2$·4H$_2$O (p.a.) and FeCl$_3$·6H$_2$O (99.7 %) salts were purchased from Anedra (Research-AG) and Supelco (Merck), respectively. Tetraethyl orthosilicate (TEOS, 99 %) was acquired from Sigma-Aldrich. Ammonium hydroxide (NH$_4$OH, 25 % wt) was obtained from Ciccarelli. Absolute ethanol (≥99.5 % V/V), EDTA (ethylenediaminetetraacetate, p.a) and isopropanol (catalog number: 2000971600) was purchased from Biopack. Guanidinium thiocyanate (catalog number: G9277) for molecular biology with a purity of ≥99 % was purchased from Sigma-Aldrich. Triton X-100 (catalog number: TB0198), of biotech grade, was acquired from BioBasic. Tris HCl buffer was prepared using Tris (Tris-Hydroxymethyl-aminomethane, catalog identifier: RU2510) with a purity of ≥99 %, purchased from

GenBiotech, and HCl (catalog number: 918, 36.5–38.0 % Pro-analysis) was obtained from Ciccarelli. DTT (DL-Dithiothreitol; Cleland's reagent) was purchased from Thermo Scientific. Trypsin and Minimum Essential Medium (MEM) from Gibco™ and fetal bovine serum (code: FBI) from Internegocios S.A. were used for assays involving A549 cells. All chemicals were used as received. Experiments were conducted using ultrapure water (EMD Millipore, USA).

2.2. Preparation of MNPs@SiO$_2$ magnetic beads

Magnetic Fe$_3$O$_4$ nanoparticles (core, MNPs) were prepared by co-precipitation method from a mixture of Fe(II) and Fe(III) (1:2 M ratio) upon addition of NH$_4$OH [20]. For example, to prepare a stock solution of MNPs, 2.75 g of FeCl$_3$.6H$_2$O were mixed with 1.02 g of FeCl$_2$.4H$_2$O and 100 mL of deionized water in a round bottomed flask under N$_2$ flow. 75 mL of NH$_4$OH (25 %wt) was added to the mixture dropwise and left under constant stirring for 1 h. The resulting black product (bare MNPs) was collected with a magnet, washed several times with deionized water and resuspended in 50 mL of it. The SiO$_2$ functionalization was achieved by the hydrolysis of TEOS, following the protocol provided in Ref. [5] after slight modifications. Briefly, to prepare a stock of MNPs@SiO$_2$ beads, 5 mL of freshly prepared MNPs were washed with ethanol and resuspended in 150 mL of ethanol by sonication. After adding 3.8 mL of NH$_4$OH and 3.4 mL of TEOS that were added dropwise, the mixture was homogenized for several minutes and heated to 80 °C. After adding 25 mL of H$_2$O the mixture was left stirring for 4 more hours, allowing the formation of silica layers on the surface of MNPs. Afterward, the silica-coated MNPs were collected with a magnet and then washed with ethanol first and then deionized water several times to remove residual TEOS and finally suspended in 10 mL of ultrapure water and kept at 4 °C for further use.

2.3. Magnetic beads characterization

The MNPs@SiO$_2$ total concentrations (wt/vol) in the colloids were estimated from the weighted mass of dried samples, and the Fe concentration in the samples was determined by means of the so-called thiocyanate method [21]. Briefly, samples (MNPs and MNPs@SiO$_2$) were treated with aqua regia (an oxidizing mixture of nitric acid and hydrochloric acid in 1:3 M ratio) in order to oxidize and dissolve the iron species. The resulting solution was heated in order to eliminate the excess acids and oxidant gasses (Cl$_2$, NOCl, NO,and NO$_2$). Then, after dilution to a fixed volume, an excess of KSCN was added in order to form Fe(III) thiocyanate red-colored complexes, in our case the predominant complex is [Fe(SCN)$_6$]$^{3-}$. The Fe(III) concentration of the solution was determined by measuring the absorbance at 480 nm employing a Shimadzu UV-2600 spectrophotometer. A calibration curve was constructed dissolving known amounts of pure Fe powder (purity was checked by ME spectroscopy), which were subsequently treated in the same way as described for nanoparticles. SiO$_2$ concentration was estimated by subtracting Fe$_3$O$_4$ concentration obtained by UV–Vis from the total concentration determined by the weighted mass of dried samples and was corroborated with the vibrating sample magnetometer (VSM) and magnetic force measurements.

The morphology and microstructure of silica-coated magnetic particles were characterized by Scanning Electron Microscopy (SEM) and Scanning Transmission Electron Microscopy (STEM). Secondary electron images were obtained in a SCIOS 2 FESEM microscope from FEI Thermo Fisher Scientific at 2 kV. High-angle annular dark field (HAADF) images and Si, Fe energy-dispersive X-ray spectroscopy (EDS) maps were acquired in STEM mode by using an FEI TALOS F200X G2 microscope. The samples were prepared by drying 10 µL of diluted colloids on a C-covered Cu grid. Dynamic light scattering (DLS, Malvern ZetasizerNanoZS) was used to measure the hydrodynamic size and Z-potential. To this end, the stock magnetic particles dispersion was diluted with ultrapure water to reach 0.4 mg/mL, shaking vigorously in a vortex mixer. The measurement time was adjusted to avoid the precipitation of particles during the assay.

Additionally, bead sizes were determined from microscopic observations. For this purpose, a drop of ferrofluid was dried from a microscope slide and observed using a Leica DM IL LED 1000 microscope with a Nikon D3100 camera attached. The photos obtained were analyzed using *ImageJ* software [22]. Ellipses shapes were manually drawn on 102 particles, and the mean radius of each particle was collected. Mean value and standard deviation were obtained from this set of values, in addition, the particle size histogram was fitted with a log-normal function using an ad-hoc *python* script and *lmfit* package [23].

The magnetic properties of bare MNPs and MNPs@SiO$_2$ samples were investigated using a Lake Shore 7400 vibrating sample magnetometer (VSM). Hysteresis loops were taken at room temperature with a maximum applied field of 1.9 T. Additional measurements of the response of the samples to a magnetic force were performed to quantify the effectiveness of these particles to be collected during the purification process. To this end, the force exerted by a Nd$_2$Fe$_{14}$B magnet (diameter 5 cm, 1.2 cm height) on each sample at a distance of 5 mm (magnetic field strength of 240 mT and magnetic field gradient of 10.5 mT/mm) was determined using an analytical balance (RADWAG PS 1000/C/2). The results are reported as magnetic force per unit weight (dimensionless). Each sample was measured twenty times, and the result reported is the mean value and the variance.

2.4. Cell culture

A549 (ATCC CCL-185) cell monolayers were grown in flasks containing minimum essential medium (MEM) supplemented with 10 % fetal bovine serum. A549 cells were harvested using 1 % trypsin-EDTA in PBS (Phosphate Buffered Saline) and incubated at 37 °C with a 5 % CO$_2$ in the air atmosphere. Cells were counted in a Neubauer chamber, resuspended in PBS and transferred to an Eppendorf tube at a final concentration of 5 × 10^5 cells/ml.

2.5. Swab samples and RNA extraction

Swab samples were collected between March and July 2020. These samples were randomly chosen from patients residing in different cities of Buenos Aires Province who had symptoms associated with respiratory diseases but did not have a confirmed diagnosis of COVID-19. RNA extraction of swab samples was performed in three diagnostic laboratories located in Buenos Aires Province, Argentina: Rossi Hospital, Public Health Laboratory (Facultad de Ciencias Exactas, Universidad Nacional de La Plata), and Evita Hospital. Upon arrival, nasopharyngeal and oropharyngeal swab samples preserved in PBS or saline were properly stored at 4 °C in case of immediate use or kept at −70 °C until further processed. Every sample under analysis was split into two aliquots of identical volume; for one aliquot RNA was isolated using the magnetic beads purification method: Magnetic Beads - UNLP (MB-UNLP), and the other fraction by using a commercial method: Viral Nucleic Acid Extraction Kit column method; GeneAid Biotech (Taiwan) in the cases of Rossi Hospital and Public Health Laboratory, or the Abbott Magnetic Beads Abbott Molecular Inc.(Des Plaines, IL, USA) in the case of Evita Hospital. In order to ensure the reliability of the results and the reproducibility of the method, the determinations were made simultaneously using both methods, and they were performed by different technicians.

This study was conducted in the context of a pandemic, during which laboratories were processing hundreds of clinical samples daily. Therefore, the number of samples included was limited. However, it is important to note that these samples were obtained from patients with suspected COVID-19 that were randomly selected. The assays were performed by different operators in different laboratories, ensuring diverse perspectives and minimizing the likelihood of sampling biases.

2.6. RNA extraction by column method

In cases where the Viral Nucleic Acid Extraction column method was used for cell culture RNA extraction, the procedure was carried out following manufacturer's instructions (GeneAid Biotech, Taiwan) [24].

2.7. RNA extraction protocol by MB–UNLP method

To isolate total RNA from biological samples, a lysis buffer containing 4 M of guanidinium thiocyanate, 2 % Triton X-100, Tris HCl 50 mM (pH 7.6–8) and 20 mM EDTA (ethylenediaminetetraacetate) was used (in case of swab samples, 750 μL of 1 mM DTT were added to 10 mL of lysis buffer); the pH of the lysis buffer was adjusted to 6.5. Then, 200 μL of lysis buffer and 200 μL of the sample (A549 cells in phosphate-buffered saline -PBS- or nasopharyngeal swab) were mixed in a 1.5 mL Eppendorf tube by pipetting or vortexing and incubated at room temperature for 10 min. Subsequently, 400 μL of isopropanol was added to the tube, mixed by vortexing, and then 40 μL of magnetic particle suspension (10 mg/mL) was added, mixed, and incubated for 5 min at room temperature. Tubes were placed in a magnetic rack until the solution was clarified, and the supernatant was discarded. MNPs@SiO$_2$ were washed with 150 μL of isopropanol. A final wash with 200 μL of 80 % ethanol was performed. Ethanol was air-dried, and 50 μL of RNase-free water was added to each sample and incubated for 5 min at room temperature to elute the nucleic acids. Finally, the supernatant was transferred to a new tube and stored at −80 °C until use, or immediately used for gel electrophoresis, spectrophotometry or qRT-PCR. A more detailed protocol is provided in Supplementary Information Additional File 1 (Protocol).

2.7.1. Assessment of yield and quality of RNA samples

To determine the quantity and quality of the RNA samples, a NanoDrop 2000 spectrophotometer (Thermo Scientific) was used. Briefly, 1 μL of each sample was pipetted onto a measured pedestal and the concentration of the RNA sample was calculated using software associated with the instrument, which is based on the Lambert-Beer equation to correlate the measured absorbance with concentration. To assess the purity of samples, the ratio of absorbance at 260 nm vs. absorbance at 280 nm was determined. Generally, ratios around 2 are taken as a purity criterion for RNA. Abnormal ratios may indicate the presence of protein or other contaminants such as guanidine. As a blank solution, RNase-free water was used. The integrity of RNA samples was analyzed by agarose gel electrophoresis. Fifteen μL of each sample, mixed with 6X loading buffer, were added to a 1.5 % w/v agarose gel containing ethidium bromide and ran for 40 min at 70 V. After separation, the resulting RNA bands were revealed under UV light.

2.8. Quantitative real time PCR (qRT-PCR)

qRT-PCR was used to detect target sequences in the purified RNA samples. Briefly, the process involves the reverse transcription of the RNA into cDNA, which is then subsequently amplified and detected using specific primers and labeled probes. During the PCR extension step, the increase of fluorescent signal is monitored by the qRT-PCR instrument (Agilent AriaMx System; Applied Biosystems, Santa Clara CA, USA) giving an amplification curve. The PCR cycle at which fluorescence rises above threshold background levels designated "threshold cycle" (Ct increases with a decreasing amount of the RNA template [25]). Here, Ct values were used to compare the performance of different RNA extraction methods. Negative controls (without RNA template) were performed in order to detect contaminants in each reaction.

2.8.1. qRT-PCR of cell culture samples

Ten μL of a 1:5 dilution of the RNA purified from A549 cells using the MB-UNLP method or the Viral Nucleic Acid Extraction Kit (GeneAid Biotech, Taiwan) were used to perform the qRT-PCR reactions using the Real-Time Fluorescent RT-PCR Kit (BGI, Taiwan) to amplify the human β–actin gene according to the manufacturer's protocol. The reverse transcription step at 50 °C for 20 min was

followed by a denaturing step at 95 °C for 10 min followed by 40 cycles of denaturation at 95 °C for 15 s, then annealing and an extension step at 60 °C for 30 s using an Agilent AriaMx System (Applied Biosystems, Waltham, MA, USA). Hex fluorescence channel was used in the detection of β–actin gene. Reactions were performed by duplicate for each RNA sample and a negative control without a template was included. Agilent Aria Software v1.5 (Applied Biosystems) was used for data analysis.

2.8.2. Detection of SARS-CoV-2

SARS-CoV-2 RNA was detected using qRT-PCR with either Discovery SARS-CoV-2 RT PCR Detection Kit (Safecare Biotech Hangzhou Co. Ltd., China) (Rossi Hospital), BGI Real-Time Fluorescent RT-PCR Kit (BGI, China) (Public Health Laboratory, UNLP) or the GeneFinder COVID-19 Plus RealAmp Kit (OSANG Healthcare, South Korea) (Evita Hospital). A sample was classified as detectable (D) or not detectable (ND) according to the criteria established by each laboratory (cycle threshold (Ct) of ORF1ab gene <38 in both Evita and Rossi Hospitals; Ct < 35 in Public Health Laboratory). Reactions were performed by duplicate for each RNA sample. Negative controls (distilled water without a template) and positive controls (pseudovirus included in each kit) were included in each qRT-PCR run.

2.9. Data analysis

Cohen's kappa coefficient (κ) was calculated as (pO-pE)/1-pE (pO is the relative observed and pE is the hypothetical probability of chance agreement). κ lower than 0 denoted a "poor", from 0 to 0.20 a "slight", from 0.21 to 0.40 a "fair", from 0.41 to 0.60 a "moderate", from 0.61 to 0.80 a "substantial", and from 0.81 to 1.00 an "almost perfect" agreement [26]. Cohen's kappa values were calculated with 95 % of Confidence intervals (CIs) and a p-value <0.05 were considered significantly. The statistical analyses were conducted with IBM SPSS (Statistical Package for the Social Sciences). Specificity and sensitivity of the MB-UNLP method were calculated according to the method proposed by Pita Fernández and collaborators [27].

2.10. Ethical statements

Ethical approval was not required for the study of anonymous swab samples, in accordance with the local legislation and
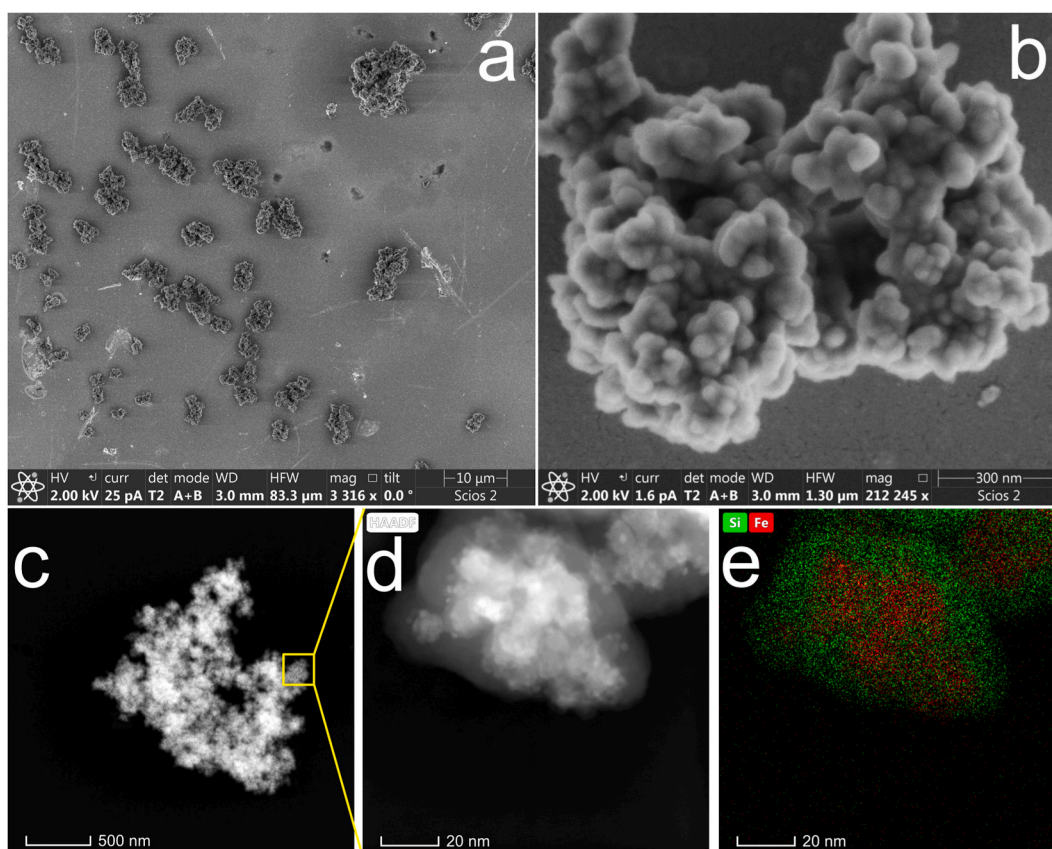

Fig. 1. **(a)** MNPs@SiO$_2$ 3720 SEM micrograph shows the formation of irregular clusters with micrometric size. **(b)** A single MB composed of several MNPs. **(c–d)** HAADF-STEM images of a single MB. **(e)** Si and Fe EDS elemental mapping reflecting the SiO$_2$ coverage on the MNPs.

institutional requirements.

3. Results and discussion

3.1. Physicochemical characterization

Several batches of MNPs and MNPs@SiO₂ were prepared following the procedure described above. The diameter of MNPs determined by STEM was 15–20 nm but the hydrodynamic diameter due to MNPs aggregation was around 700 nm. The particle morphology of MNPs@SiO₂ is displayed in Fig. 1. Each MNPs@SiO₂ exhibited an irregular morphology (Fig. 1a); a closer inspection of the clusters showed that these are composed of several bare MNPs (Fig. 1b). The aforementioned fact can be corroborated by STEM-HAADF images and EDS elemental maps shown in Fig. 1(c-e). Since the intensity in STEM-HAADF images increases with the atomic number of the elements, the brightest zones correspond to Fe while the lighter ones account for Si; in this regard, see the EDS elemental map, Fig. 1e. An average hydrodynamic diameter of 2.0 μm of MNPs@SiO2 particles was determined by DLS analysis (not shown here).

Furthermore, particle size was determined through microscopic observations (Fig. 2a), where a dried drop of MNPs@SiO2 particles is depicted. Using ImageJ software, 102 particles were manually outlined with ellipses. The resulting histogram, illustrating the distribution of particle sizes, is presented in Fig. 2b. The diameter used corresponds to that of a circle with the same area as the manually drawn ellipses around each particle. A log-normal distribution was fitted, yielding a mean diameter of 1.4 μm with a standard deviation (σ) of 0.17 μm.

The mass percentage of silica in the MNPs@SiO₂ is strongly dependent on the synthesis condition during the TEOS hydrolysis process. When ammonium and ethanol are allowed to evaporate during the process, the amount of silica is higher than if the seal were hermetic. Then, MNPs@SiO₂ with different silica mass percentages can be obtained using the same amounts of reactants depending on the setup of the experiment. When the hydrolysis took place in an open round-bottomed flask, the SiO₂ amount was about 10 % while using a coolant to prevent solvent evaporation, a percentage up to 60 % was reached. When the reaction was left overnight (23 h), 77 % SiO₂ was obtained. On the other hand, the Zeta potential of MNPs@SiO₂ particles measured was negative with values between −49.6 and −20 mV, being more negative when the silica concentration increased (see Fig. 3d).

The magnetization cycles of four different samples were analyzed (Fig. 3a). Two of them correspond to bare nanoparticles and the remaining ones are nanoparticles coated with different percentages of silica. The saturation magnetization (M_S) of MNPs is about 70 emu/g, while the remanence and coercivity are almost zero, as expected for the single magnetic domain in the superparamagnetic regime. On the other hand, the magnetic force measured for MNPs is about 60 times its weight.

The saturation magnetization of MNPs@SiO₂ exhibited a linear decay relationship with the amount of silica, see Fig. 3b. Note that the lower the percentage of silica, the saturation magnetization tends to the value of the MNPs, indicating that the coating does not affect the magnetic core and that the M_S linear detriment is only related to the mass normalization. Also, the magnetic force as a function of SiO₂ percentage displayed a similar performance to that exhibited for the M_S versus SiO₂ percentage (Fig. 3c). In order to find the optimal characteristics of the material for the application, it seems that there is a compromise between higher colloidal stability with a higher amount of SiO₂ (Z-potential more negative) and a higher magnetic force for a smaller amount of SiO₂. In view of this, three batches with SiO₂ percentages between 40 and 60 % were selected.

3.2. RNA isolation from A549 cell cultures

To assess the performance of the MB–UNLP method for RNA extraction, A549 cells derived from human lung carcinoma were used.
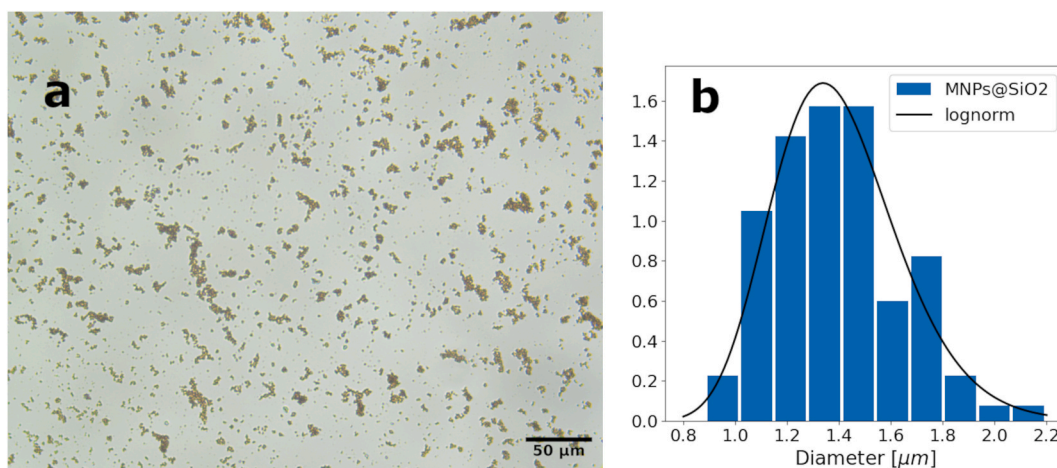

Fig. 2. **(a)** Microscope photography taken to calculate size distributions of MNPs@SiO2. Ellipses were drawn manually with ImageJ software. **(b)** Histogram of particle size distribution obtained from the ellipses data. The number of particles analyzed was 102.
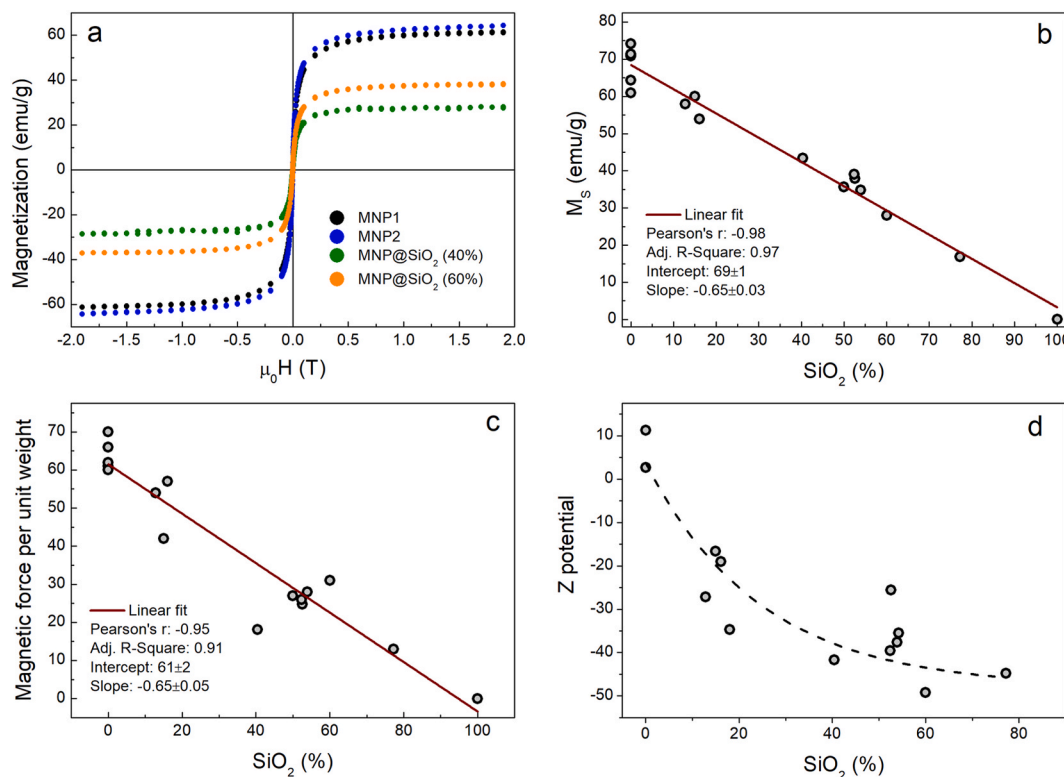
Fig. 3. (a) Magnetization curves for bare MNPs (black and red circles) and silica-coated MNPs@SiO$_2$ (green and blue dots). MNPs exhibit similar saturation magnetization values while in coated particles the magnetization decreases with increasing silica percentage. **(b)** Evolution of saturation magnetization as a function of silica percentage. **(c)** Magnetic force per unit weight (dimensionless) versus silica percentage. **(d)** Z potential a function of silica percentage, the dash-dotted line is only to guide the eye.

MNPs@SiO$_2$ were tested using a protocol that involves a step of biological sample solubilization in a lysis buffer, binding of the particles to RNA, isopropanol and ethanol washes and resuspension of the purified RNA in double distilled water as shown in Fig. 4 panel a and detailed in Methods. Three different batches of MBs were studied and compared with a commercial method involving columns. Purified RNA samples were quantified with a spectrophotometer, and the quality was studied. Obtained ratios of absorbance at 260 and 280 nm (A260/A280) were similar between the two methods and comparable among MBs batches with values around 2, indicating the RNA purity (Fig. 4, panel b). Furthermore, reproducibility within 3 different batches of MBs was appreciated, as band intensities were similar for all the extractions (Fig. 4, panel c). In order to test if the quality and quantity of the RNA samples obtained were enough for qRT-PCR, they were tested as a template for the human β–actin gene amplification using specific primers and a TaqMan probe set included in the real-time PCR kit. As shown in Fig. 4, panel d, comparable Ct values were obtained using the spin column method (Ct 14.72) and MB-UNLP method (Ct 15.10 ± 0.20). In parallel, the MB-UNLP method was tested on other types of samples, such as insects and different types of tissues and accurate results were obtained [28].
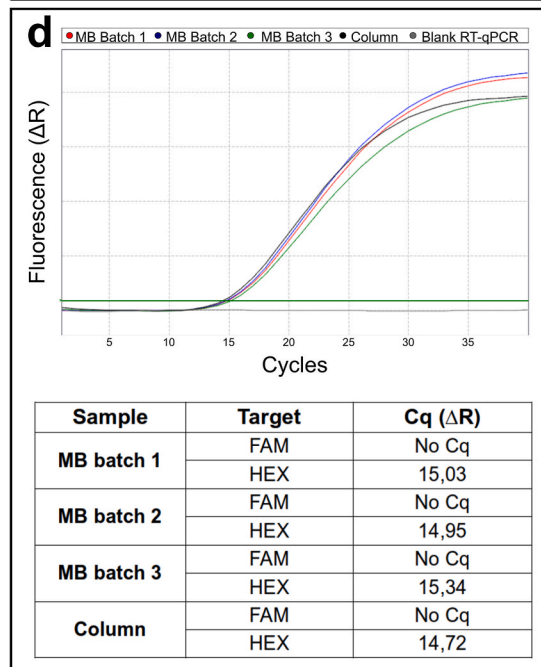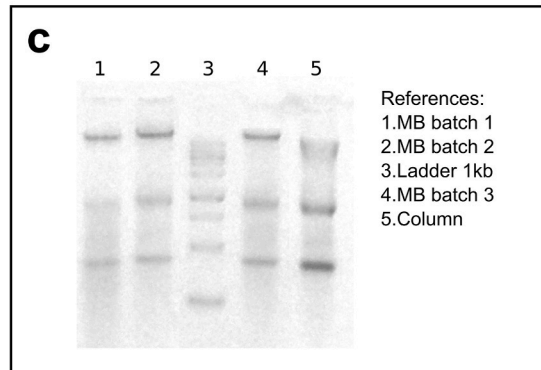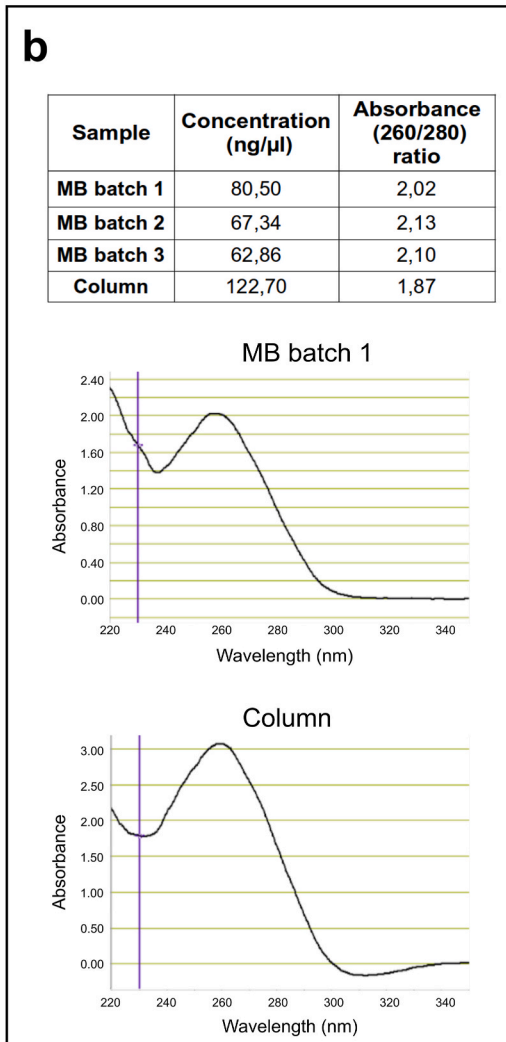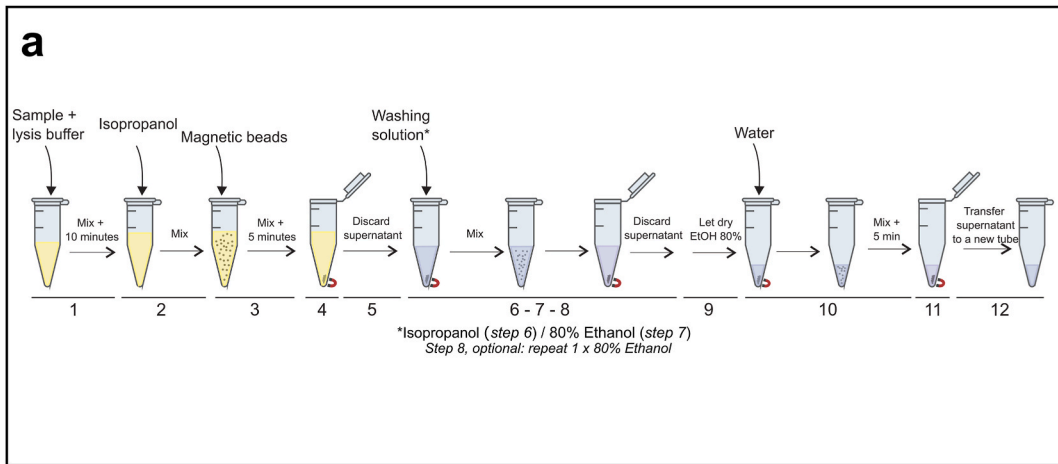
3.3. Evaluation and validation of the MB–UNLP method in the purification of SARS-CoV-2 RNA

3.3.1. Rossi Hospital
A total of 30 samples were processed in parallel by the MB-UNLP and column methods. The internal control gene RNase P was detected in all samples (Fig. 5a) with a ΔCt value (Ct MB-UNLP – Ct Genaid columns) of 3.8 (±1.92) (Table 1). For the ORF1ab gene, ND and D samples gave 100 % of coincidence among comparative RNA extraction methods (Fig. 5b) with a ΔCt of 5.13 (±2.93) (Table 1). Kappa coefficient calculation was 1 (observed agreement 100 %, confidence interval 95 %) obtaining 'almost perfect agreement' among methods as shown in Table 1. Supplementary Table S1.1 provides data on Ct and comparative results. The sensitivity and specificity of MB-UNLP method were 100 % (95 % CI, 69.87 %–99.23 %) and 100.00 % (95 % CI, 78.12–99.49 %), respectively (Supplementary Table S2.1).

3.3.2. Public Health Laboratory
Forty-six nasopharyngeal swab samples were processed by the MB-UNLP method and the columns in parallel. Ct values obtained for the internal control gene β-actin showed a ΔCt value (Ct MB-UNLP – Ct Genaid columns) of 1.8 (±1.1). Positivity in samples was detected with a 100 % of coincidence (Fig. 5c and Table 1). Ct values for the ORF1ab gene, indicate a 96.77 % coincidence in the ND (*i.*

a

Sample + lysis buffer → Mix + 10 minutes | Isopropanol → Mix | Magnetic beads → Mix + 5 minutes | Discard supernatant | Washing solution* → Mix | Discard supernatant | Let dry EtOH 80% | Water → Mix + 5 min | Transfer supernatant to a new tube

1   2   3   4   5   6 - 7 - 8   9   10   11   12

Isopropanol (step 6) / 80% Ethanol (step 7)
Step 8, optional: repeat 1 x 80% Ethanol

b

Sample	Concentration (ng/μl)	Absorbance (260/280) ratio
MB batch 1	80,50	2,02
MB batch 2	67,34	2,13
MB batch 3	62,86	2,10
Column	122,70	1,87

c

References:
1. MB batch 1
2. MB batch 2
3. Ladder 1kb
4. MB batch 3
5. Column

d

Sample	Target	Cq (ΔR)
MB batch 1	FAM	No Cq
	HEX	15,03
MB batch 2	FAM	No Cq
	HEX	14,95
MB batch 3	FAM	No Cq
	HEX	15,34
Column	FAM	No Cq
	HEX	14,72

(caption on next page)

Fig. 4. (a) Schematic representation of RNA extraction protocol by the MB–UNLP method. The numbers below correspond to the extraction steps, which are described in detail in Supplementary file 1. **(b)** Quantification of RNA samples by Nanodrop™ and UV absorption spectra (typical spectra are presented) to determine the absorbance ratios at 260 and 280 nm (A_{260}/A_{280} ratio). **(c)** Lines 1, 2, and 4 correspond to RNA extractions using three batches of MBs; lane 3 is the 1 kb ladder (Guangzhou Dongsheng Biotech, R.P. China), and lane 5 corresponds to RNA extraction using the GeneAid kit column method. The original gel is provided in "Supplementary Information". **(d)** Comparative qRT-PCR results of RNA extraction and amplification curves of the human β–actin gene in RNA samples purified either with different MBs batches or Viral Nucleic Acid Extraction Kit column method (GeneAid Biotech, Taiwan). The horizontal line represents the fixed threshold chosen for the analysis.

e. not detectable) samples (one sample reported as ND by the Geneaid column method, was considered detectable by the MB-UNLP method) (Fig. 5d and Table 1) and an 86.67 % coincidence in D samples (two D samples using the Geneaid columns were considered ND with MB-UNLP) (Fig. 5d and Table 1), obtaining a ΔCt of 1.2 (±2.4) for the viral gene. Agreement between methods was 'almost perfect' obtaining a Kappa coefficient of 0.802 (±0.091; observed agreement 93.48 %, confidence interval 95 %: 0.684 to 1.000) (Table 1). Table S1.2 provides data on Ct and results among methods. Our method showed a sensitivity of 86.67 % (95 %CI: 58.39 %–97.66 %) and a specificity of 96.77 % (95 % CI:81.49 %–99.83 %) in the detection of SARS-CoV-2 as it was shown in Supplementary Table S2.2.

3.3.3. Evita Hospital

Forty-six samples were processed in parallel by the MB-UNLP and the Abbott MB. The internal control RNase P was detected with a 100 % coincidence, showing a ΔCt of 0.16 (±0.95) (Fig. 5e and Table 1). The Ct value for the ORF1ab gene (Fig. 5f and Table 1), indicates an 80 % of coincidence in the ND samples and 66.67 % for D samples, with a ΔCt of −0.06 (±0.92) (Fig. 5e Table 1). Kappa index obtained 0.431 (±0.143; observed agreement 76.60 %, confidence interval 95 %: 0.151 to 0.711) indicates 'moderate agreement' among methods. Specificity obtained was 87.50 % (95 % CI: 70.07 %–95.92 %) and the sensitivity was 57.14 % (95 % CI: 29.65 %–81.19 %). In comparison to other health centers, the concordance value (K) and sensitivity of the proposed method were lower. This discrepancy can be attributed to the samples that were detected as positive by the MB-UNLP method but reported as negative by the Abbott method (Fig. 5f). For these 7 samples, the presence of SARS-CoV-2 should have been further evaluated using a third method. Additional data, including Ct values and results among methods, are available in Table S1.3 and Table S2.3.

3.4. Comparison of nucleic acid extraction methods for RNA purification in COVID-19 diagnosis

Recently, many methods for nucleic acid extraction based on magnetics beads were developed. Klein and collaborators [18] proposed an optimized protocol for 96-well plates allowing the rapid processing of multiple samples by using the manual pipetting system Liquidator 96. However, authors have stated that transferring samples from swab tubes to 96-well plates is a time-consuming and laborious step, thereby increasing the total operation time. Furthermore, the use of multi-well plates implies the need to collect a certain quantity of samples to optimize the use of the resources, as the plates cannot be reused. A promising method based on poly-(amino ester) with carboxyl group (PC)-coated magnetic nanoparticles, was performed to purify RNA in less than 9 min. However, the preparation of polymer-coated magnetic beads is a laborious process that involves many steps. In addition, the method was assayed on SARS-CoV-2 pseudovirus particles and remains to be tested on human samples [29].

Also, a low-cost protocol based on magnetic nanoparticles prepared from bacterial biofilm waste was developed. Nevertheless, the method requires sophisticated lab equipment to obtain the MNPs from biowaste by heating at very high temperatures [30]. Finally, Sossai Possebon and collaborators [31] developed a method for RNA extraction using a similar lysis buffer with guanidinium thiocyanate. However, the protocol is based on commercial magnetic beads, increasing the cost of the assay (0.68 USD per reaction vs 0.043 USD obtained with MB-UNLP method) and making it impossible to adapt the method for local manufacturing.

Results indicate that MB-UNLP method is a reliable option for RNA purification from swab samples for COVID-19 diagnosis. Although sensitivity yielded varies between the different centers of diagnosis, the results obtained are comparable with the Trizol RNA extraction method (96 %), the heat shock technique (82.6 %) and the column method (100 %) [32,33]. Compared with other protocols that are generally used for nucleic acid isolation, our protocol proved to have a lower cost per determination (0.043 US/reaction) than those involving Trizol (0.7 US/reaction) or columns (4.25 US/reaction). It is also faster, with a total duration of 40 min, against 60 and 95 min of columns and Trizol methods, respectively. Furthermore, these extraction methods are based on the use of buffers or reagents that cannot be easily replaced, since their composition is undisclosed and, hence, they are not easily accessible worldwide, or they cannot be acquired individually. In a high-demand context (such as a Pandemic or outbreak) or under economic resource limitations, the nanoparticle based methodology reported here ensures sustainability by minimizing the use of costly buffers or reagents, making it more affordable and accessible. Also, the nanoparticle method can be adapted to local production in Low and Middle Income countries.

Although heat shock represents a fast, simple and cheap strategy for RNA preparation from different biological samples for RT-PCR amplification, degradation cannot be ruled out during the process. Also, less sensitivity was observed compared with purified samples [34]. Thermal shock can lead to the cleavage of RNA into shorter fragments, reducing the overall RNA content. This phenomenon has been reported in several studies [35–37]. It is possible that samples with lower viral loads (fewer RNA copies) such as those early in infection could be more prone to yield false-negative results when testing for the presence of the virus. Moreover, the method is limited to one type of sample (swabs).

In contrast to the other alternatives, the MB-UNLP method does not need expensive laboratory instrumentation, and processing multiple samples can be easily automated (**Table 2**).
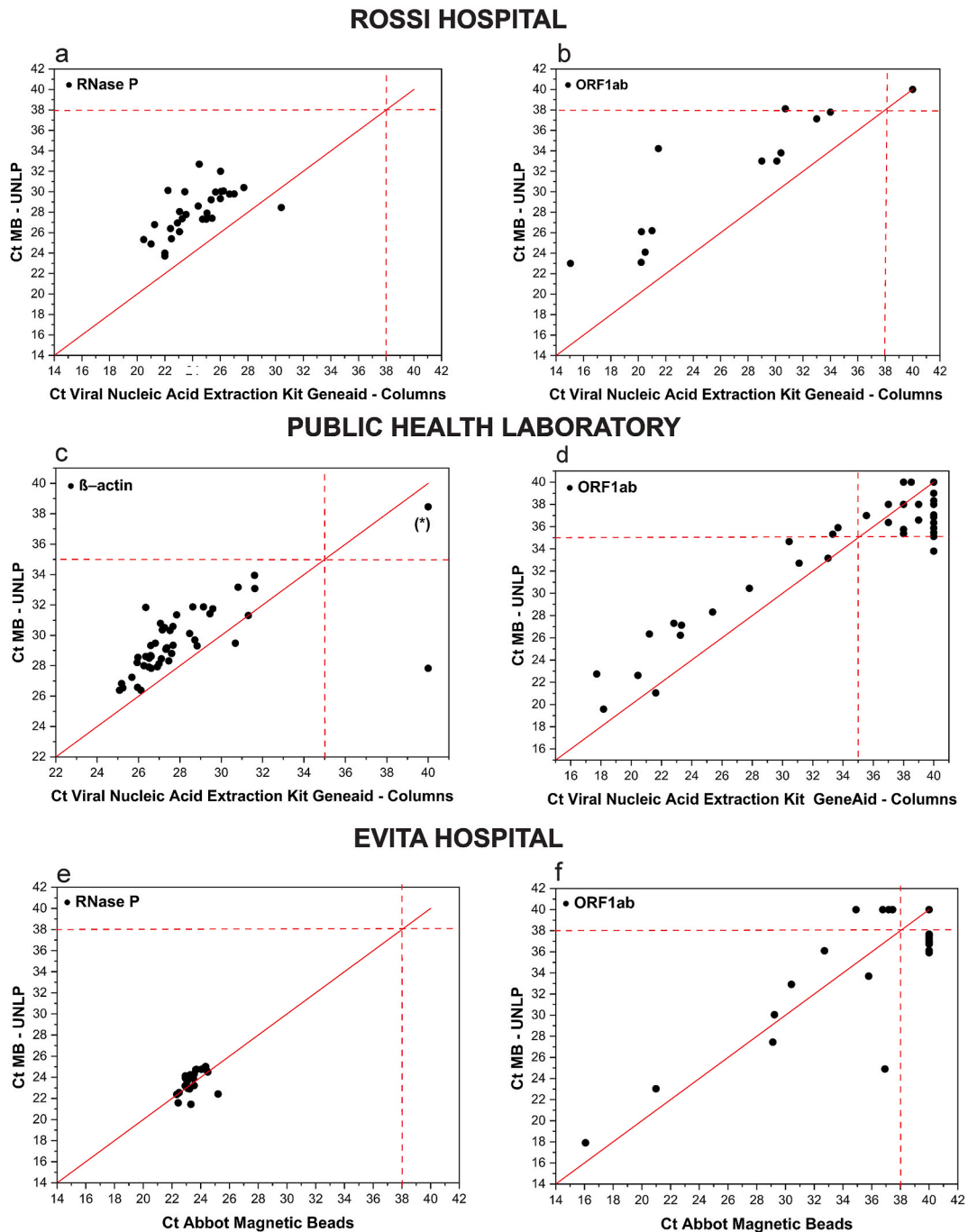
ROSSI HOSPITAL

PUBLIC HEALTH LABORATORY

EVITA HOSPITAL

Fig. 5. Scatter plot of the SARS-CoV-2 detection by qRT-PCR and comparison among commercial RNA extraction methods and MB–UNLP methodology. Cts obtained by the alternative commercial method are represented on the horizontal axis, and MB–UNLP Cts are represented on the vertical axis. For each panel, the upper left quadrant indicates D by both methods, the upper right quadrant indicates ND by both methods; the bottom left quadrant indicates D by a commercial method and ND by MB–UNLP, and the bottom right quadrant indicates D by MB–UNLP and ND by the commercial method. The full red line represents positions of identical Ct for both methods; the red dashed line represents the Ct limit established by each laboratory. **(a)** and **(b)** Rossi Hospital Ct results for the internal control RNase P and ORF1ab gene (N = 30); **(c)** and **(d)** Public Health Laboratory Ct results for the internal control β-actin and ORF1ab gene (N = 46, * indicates negative control); **(e)** and **(f)** Evita Hospital Ct results for the internal control RNase P (N = 24) and the ORF1ab gene (N = 46).

Table 1

Overall performance of the RNA extracted with the MB – UNLP methodology in the detection of SARS-CoV-2: comparative test results and analysis in three diagnostic laboratories with RNA extracted by the commercial method used in each laboratory and RNA extracted with MB from the same swab samples * indicates a p - value close to "0", so with high significance.

		Rossi Hospital	Public Health Laboratory	Evita Hospital
Samples	**Detected**	12/12 (100 %)	13/15 (86.67 %)	8/12 (66.7 %)
	No detected	18/18 (100 %)	30/31 (96.77 %)	28/34 (82 %)
Number of observed agreements (% of the observations)		30 (100 %)	43 (93.48 %)	36 (76.60 %)
Cohen's kappa coefficient (κ) ($\pm$SE)		1	0.85 ($\pm$0.084)	0.43 ($\pm$0.143)
p - value		<0.05*	<0.05*	0.03
95 % confidence interval		1.000 to 1.000	0.684 to 1.000	0.151 to 0.711
Number of agreements expected by chance		15.6 (52 % of the observations)	26.1 (56.81 % of the observations)	27.7 (58.85 % of the observations)
ΔCt	**Internal Control**	3.8 ($\pm$1.92)	1.8 ($\pm$1.1)	0.16 ($\pm$0.95)
	ORFa1	5.3 ($\pm$2.9)	1.2 ($\pm$2.4)	−0.06 ($\pm$0.92)

Table 2

Comparison of the MB-UNLP method and other methods usually used for ribonucleic acid purification: summary table with a comparative of technical characteristics of different RNA extraction methodologies and the MB-UNLP method.

Method	Trizol	Columns	Heat shock	MB-UNLP
Steps	Lysis sample and separate phases	Lysis	Heat treatment	Lysis
	Precipitate the RNA	Nucleic Acid Binding	Incubation 4 °C	Nucleic Acid Binding
	Wash the RNA	Wash		Wash
	Solubilize the RNA	Elution		Elution
		Nucleic Acid Concentration		
Starting material	Serum, plasma, body fluids, different types of tissues and the supernatant of viral infected cell cultures.	Different types of tissues, cell culture	Limited to swabs	Naso- and Oro- pharyngeal swabs, different types of tissues, cell culture
Equipment	Centrifuge and rotor capable of reaching 12,000×g and 4 °C	Centrifuge and rotor capable of reaching 12,000×g and 4 °C	Thermal cycler 95/98°	Magnetic Rack
	Water bath or heat block at 55–60 °C	Water bath or heat block at 65 °C	Block at 4 °C	
Reagents	Trizol		None	
	Isopropanol	Commercial buffers		Buffer GITC
	Ethanol, 75 %	Absolute ethanol		Isopropanol
	Chloroform	Isopropanol		Ethanol, 80 %
Cost per determination (US/reaction)	0.7	4.25		0.043
Operation time	95 min	60 min	10 or 20 min	40 min
Possibility of Automatization	No	No	No	Yes
Reference	[38,39]	[24,40]	[34,36]	[11,28]

4. Conclusions

Since the declaration of COVID-19 as a pandemic in 2020, more than 700 million cases have been reported globally [41]. Three years later, RT-qPCR continues being the gold standard for SARS-Cov-2 detection due to its sensitivity and specificity. Although protocols that avoid RNA isolation have been described, RNA purification warrants more reliable results [42].

In this study, a method for RNA extraction (MB-UNLP method) based on the use of magnetic microparticles was optimized in order to achieve a satisfactory RNA yield and purity for the detection of SARS-CoV-2 in oro- and nasopharyngeal swab samples. Silica coated magnetic particles were successfully synthesized by coprecipitation followed by hydrolysis of tetraethyl orthosilicate and its performance for RNA purification was evaluated. As part of the physicochemical characterization, particles' hydrodynamic size and negative Z potential were determined by light scattering. Morphology studies by SEM exhibited the formation of irregular clusters with micrometer-sized particles, and that each microparticle was composed of several bare nanoparticles. Finally, samples presented an appropriate magnetic response maintaining their superparamagnetism properties even after SiO_2 coating.

Our data demonstrate that viral RNA extraction performed with the MB-UNLP method is comparable with commercial methods, such as GeneAid columns and the Abbott robotic method using magnetic nanoparticles. Moreover, we observed robust SARS-CoV-2 qRT-PCR diagnosis results, given by rates of coincidence greater than 75 % between clinical samples processed by MB-UNLP and commercial methods. Nucleic acid purification methods are important for molecular diagnosis; in pandemic periods, when global demand is high and consumables are scarce, the local production of methods for high-throughput sample processing is crucial.

In conclusion, we propose a rapid, cost-effective and easily automatable method for RNA extraction. Although the protocol in this

study was tested for SARS-Cov-2 detection, this method could be adapted for the diagnosis of other diseases.

Ethics statement

This research was implemented since the end of May 2020 as part of surveillance activities coordinated by the Ministry of Health of the Province of Buenos Aires, following national and provincial guidance (https://www.argentina.gob.ar/salud/coronavirus-COVID-19/laboratorio, https://www.argentina.gob.ar/ciencia/seppCTI/desarrollo-tecnologico-e-innovacion/kit-de-extraccion-de-acidos-ribonucleicos-para). In accordance with the Resolution No. 908/2020 of the Ministry of Health of Argentina and the Ethical and Operational guidelines for accelerated ethics review of research involving human beings related to COVID-19 [May 2020] written informed consent of the participant's legal guardian/next-of-kin was not required to participate in the study". Samples included in section 2.5 were considered de-identified and determined to be exempt because they were not considered human subjects research due to the quality improvement and public health intent of the work.

Additional information

Fig. 4 (a) and graphical abstract were created with BioRender software, ©biorender.com.

Data availability statement

The majority of the data supporting this manuscript is provided in the supplementary materials. Additional data not included in the supplementary materials will be made available upon request. Please contact the corresponding author via email with sufficient advance notice to facilitate the timely sharing of the requested data.

CRediT authorship contribution statement

Natalia Capriotti: Writing – review & editing, Writing – original draft, Methodology, Investigation, Formal analysis, Data curation, Conceptualization. **Leslie C. Amorós Morales:** Writing – review & editing, Writing – original draft, Methodology, Investigation, Formal analysis, Data curation, Conceptualization. **Elisa de Sousa:** Methodology, Investigation, Formal analysis, Data curation, Conceptualization. **Luciana Juncal:** Methodology, Investigation, Formal analysis, Data curation, Conceptualization. **Matias Luis Pidre:** Writing – original draft, Methodology, Investigation, Formal analysis, Data curation, Conceptualization. **Lucila Traverso:** Writing – original draft, Methodology, Investigation, Formal analysis, Data curation, Conceptualization. **Maria Florencia López:** Writing – original draft, Methodology, Investigation, Formal analysis, Data curation, Conceptualization. **Maria Leticia Ferelli:** Writing – original draft, Methodology, Investigation, Formal analysis, Data curation, Conceptualization. **Gabriel Lavorato:** Methodology, Investigation, Formal analysis, Data curation, Conceptualization. **Cristian Lillo:** Methodology, Investigation. **Odin Vazquez Robaina:** Methodology, Investigation. **Nicolas Mele:** Methodology, Investigation. **Carolina Vericat:** Supervision, Methodology, Investigation, Conceptualization. **Patricia Schilardi:** Methodology, Investigation. **Alejandra Fabiana Cabrera:** Methodology, Investigation. **Silvana Stewart:** Methodology, Investigation. **Mariano H. Fonticelli:** Supervision, Methodology, Investigation. **Pedro Mendoza Zéliz:** Writing – original draft, Supervision, Methodology, Investigation, Formal analysis, Conceptualization. **Sheila Ons:** Writing – original draft, Supervision, Resources, Methodology, Investigation, Funding acquisition, Formal analysis, Data curation, Conceptualization. **Victor Romanowski:** Writing – original draft, Supervision, Resources, Investigation, Funding acquisition, Formal analysis, Conceptualization. **Claudia Rodríguez Torres:** Writing – review & editing, Writing – original draft, Supervision, Resources, Project administration, Methodology, Investigation, Funding acquisition, Formal analysis, Data curation, Conceptualization.

Declaration of competing interest

The authors declare that they have no known competing financial interests or personal relationships that could have appeared to influence the work reported in this paper.

Acknowledgments

Appendix A. Supplementary data

Supplementary data to this article can be found online at https://doi.org/10.1016/j.heliyon.2024.e25377.

References

[1] M. Yüce, E. Filiztekin, K.G. Özkaya, COVID-19 diagnosis -A review of current methods, Biosens. Bioelectron. 172 (Jan. 2021) 112752, https://doi.org/10.1016/j.bios.2020.112752 ([Not Available in CrossRef][Not Available in Internal Pubmed][Not Available in External Pubmed]).

[2] Aislamiento social. Preventivo y obligatorio., 2020. Accessed: Jul. 11, 2023. [Online]. Available: https://www.boletinoficial.gob.ar/detalleAviso/primera/227042/20200320.

[3] Ministerio de Salud, Reporte diario vespertino nro 479. Situación de Covid-19 en Argentina, Ministerio de Salud, Argentina, Reporte diario vespertino (Dec. 2020) 479 [Online]. Available: https://www.argentina.gob.ar/sites/default/files/30-12-20-reporte-vespertino-covid-19.pdf. (Accessed 11 July 2023).

[4] E.T. Beck, K.J. Henrickson, Molecular diagnosis of respiratory viruses, Future Microbiol. 5 (6) (Jun. 2010) 901–916, https://doi.org/10.2217/fmb.10.48 ([Not Available in CrossRef][Not Available in Internal Pubmed][Not Available in External Pubmed]).

[5] G. Vernet, Molecular diagnostics in virology, J. Clin. Virol. 31 (4) (Dec. 2004) 239–247, https://doi.org/10.1016/j.jcv.2004.06.003 ([Not Available in CrossRef][Not Available in Internal Pubmed][Not Available in External Pubmed]).

[6] V.M. Corman, S. Ölschläger, C.-M. Wendtner, J.F. Drexler, M. Hess, C. Drosten, Performance and clinical validation of the RealStar® MERS-CoV Kit for detection of Middle East respiratory syndrome coronavirus RNA, J. Clin. Virol. 60 (2) (Jun. 2014) 168–171, https://doi.org/10.1016/j.jcv.2014.03.012 ([Not Available in CrossRef][Not Available in Internal Pubmed][Not Available in External Pubmed]).

[7] S.Y. Kim, et al., Viral RNA in Blood as indicator of severe outcome in Middle East respiratory syndrome coronavirus infection, Emerg. Infect. Dis. 22 (10) (Oct. 2016) 1813–1816, https://doi.org/10.3201/eid2210.160218 ([Not Available in CrossRef][Not Available in Internal Pubmed][Not Available in External Pubmed]).

[8] P. Oberacker, P. Stepper, D. Bond, K. Hipp, T. Hore, T. Jurkowski, Simple synthesis of functionalized paramagnetic beads for nucleic acid purification and manipulation, BIO-Protoc. 9 (20) (2019), https://doi.org/10.21769/BioProtoc.3394 ([Not Available in CrossRef][Not Available in Internal Pubmed][Not Available in External Pubmed]).

[9] N. Kovačević, Magnetic beads based nucleic acid purification for molecular biology applications, in: M. Micic (Ed.), Sample Preparation Techniques for Soil, Plant, and Animal Samples, In Springer Protocols Handbooks, Springer New York, New York, NY, 2016, pp. 53–67, https://doi.org/10.1007/978-1-4939-3185-9_5 ([Not Available in CrossRef][Not Available in Internal Pubmed][Not Available in External Pubmed]).

[10] M. Knobel, W.C. Nunes, L.M. Socolovsky, E. De Biasi, J.M. Vargas, J.C. Denardin, Superparamagnetism and other magnetic features in granular materials: a review on ideal and real systems, J. Nanosci. Nanotechnol. 8 (6) (Jun. 2008) 2836–2857, https://doi.org/10.1166/jnn.2008.15348 ([Not Available in CrossRef][Not Available in Internal Pubmed][Not Available in External Pubmed]).

[11] R. Boom, C.J. Sol, M.M. Salimans, C.L. Jansen, P.M. Wertheim-van Dillen, J. van der Noordaa, Rapid and simple method for purification of nucleic acids, J. Clin. Microbiol. 28 (3) (Mar. 1990) 495–503, https://doi.org/10.1128/jcm.28.3.495-503.1990 ([Not Available in CrossRef][Not Available in Internal Pubmed][Not Available in External Pubmed]).

[12] S. Ghahari, S. Ghahari, G.A. Nematzadeh, Magnetic nano fluids for isolation of genomic DNA and total RNA from various prokaryote and eukaryote cells, J. Chromatogr. B 1102 (1103) (Dec. 2018) 125–134, https://doi.org/10.1016/j.jchromb.2018.10.006 ([Not Available in CrossRef][Not Available in Internal Pubmed][Not Available in External Pubmed]).

[13] A.H.F. Lee, S.F. Gessert, Y. Chen, N.V. Sergeev, B. Haghiri, Preparation of iron oxide silica particles for Zika viral RNA extraction, Heliyon 4 (3) (Mar. 2018) e00572, https://doi.org/10.1016/j.heliyon.2018.e00572 ([Not Available in CrossRef][Not Available in Internal Pubmed][Not Available in External Pubmed]).

[14] H. He, et al., Integrated DNA and RNA extraction using magnetic beads from viral pathogens causing acute respiratory infections, Sci. Rep. 7 (1) (Mar. 2017) 45199, https://doi.org/10.1038/srep45199 ([Not Available in CrossRef][Not Available in Internal Pubmed][Not Available in External Pubmed]).

[15] J. Wang, Z. Ali, J. Si, N. Wang, N. He, Z. Li, Simultaneous extraction of DNA and RNA from hepatocellular carcinoma (hep G2) based on silica-coated magnetic nanoparticles, J. Nanosci. Nanotechnol. 17 (1) (Jan. 2017) 802–806, https://doi.org/10.1166/jnn.2017.12442 ([Not Available in CrossRef][Not Available in Internal Pubmed][Not Available in External Pubmed]).

[16] Z. Zhao, H. Cui, W. Song, X. Ru, W. Zhou, X. Yu, "A Simple Magnetic Nanoparticles-Based Viral RNA Extraction Method for Efficient Detection of SARS-CoV-2," Molecular Biology, Feb. 2020, https://doi.org/10.1101/2020.02.22.961268 preprint.

[17] M.N. Esbin, O.N. Whitney, S. Chong, A. Maurer, X. Darzacq, R. Tjian, Overcoming the bottleneck to widespread testing: a rapid review of nucleic acid testing approaches for COVID-19 detection, RNA 26 (7) (Jul. 2020) 771–783, https://doi.org/10.1261/rna.076232.120 ([Not Available in CrossRef][Not Available in Internal Pubmed][Not Available in External Pubmed]).

[18] S. Klein, et al., SARS-CoV-2 RNA extraction using magnetic beads for rapid large-scale testing by RT-qPCR and RT-LAMP, Viruses 12 (8) (Aug. 2020) 863, https://doi.org/10.3390/v12080863 ([Not Available in CrossRef][Not Available in Internal Pubmed][Not Available in External Pubmed]).

[19] S.B. Somvanshi, P.B. Kharat, T.S. Saraf, S.B. Somwanshi, S.B. Shejul, K.M. Jadhav, Multifunctional nano-magnetic particles assisted viral RNA-extraction protocol for potential detection of COVID-19, Mater. Res. Innov. 25 (3) (Apr. 2021) 169–174, https://doi.org/10.1080/14328917.2020.1769350 ([Not Available in CrossRef][Not Available in Internal Pubmed][Not Available in External Pubmed]).

[20] M.E. De Sousa, et al., Stability and relaxation mechanisms of citric acid coated magnetite nanoparticles for magnetic hyperthermia, J. Phys. Chem. C 117 (10) (Mar. 2013) 5436–5445, https://doi.org/10.1021/jp311556b ([Not Available in CrossRef][Not Available in Internal Pubmed][Not Available in External Pubmed]).

[21] A.I. Vogel, G.H. Jeffery, A.I. Vogel, Vogel's Textbook of Quantitative Chemical Analysis, fifth ed., Longman Scientific & Technical ; Wiley, Harlow, Essex, England : New York, 1989 ([Not Available in CrossRef][Not Available in Internal Pubmed][Not Available in External Pubmed]).

[22] C.A. Schneider, W.S. Rasband, K.W. Eliceiri, NIH Image to ImageJ: 25 years of image analysis, Nat. Methods 9 (7) (Jul. 2012) 671–675, https://doi.org/10.1038/nmeth.2089 ([Not Available in CrossRef][Not Available in Internal Pubmed][Not Available in External Pubmed]).

[23] M. Newville, T. Stensitzki, D.B. Allen, A. Ingargiola, LMFIT: non-linear least-square minimization and curve-fitting for Python, Zenodo, Sep. 21 (2014), https://doi.org/10.5281/ZENODO.11813.

[24] Geneaid, Viral Nucleic Acid Extraction Kit II, Jul. 05, 2020 [Online]. Available: https://www.geneaid.com/Virus/VR.

[25] J. Jozefczuk, J. Adjaye, Quantitative real-time PCR-based analysis of gene expression, in: Methods in Enzymology, vol. 500, Elsevier, 2011, pp. 99–109, https://doi.org/10.1016/B978-0-12-385118-5.00006-2 ([Not Available in CrossRef][Not Available in Internal Pubmed][Not Available in External Pubmed]).

[26] J.R. Landis, G.G. Koch, The measurement of observer agreement for categorical data, Biometrics 33 (1) (Mar. 1977) 159, https://doi.org/10.2307/2529310 ([Not Available in CrossRef][Not Available in Internal Pubmed][Not Available in External Pubmed]).

[27] S. Pita Fernández, S. Pértegas Díaz, "Pruebas diagnósticas: sensibilidad y especificidad," unidad de Epidemiología clínica y bioestadística. Complexo hospitalario, universitario de A coruña. España, Cad Aten Primaria 10 (2003) 120–124, 2003.

[28] Rodriguez Torres Claudia, et al., Magnetic nanoparticles for purification of biomolecules: challenges and opportunities [Online]. Available, http://scirevfew.net/index.php/sciencereviews, 2023.

[29] H. Cui, et al., A simplified viral RNA extraction method based on magnetic nanoparticles for fast and high-throughput detection of SARS-CoV-2 ([Not Available in CrossRef][Not Available in Internal Pubmed][Not Available in External Pubmed]), Talanta 258 (Jun. 2023) 124479, https://doi.org/10.1016/j.talanta.2023.124479.

[30] L. Yu, et al., From biowaste to lab-bench: low-cost magnetic iron oxide nanoparticles for RNA extraction and SARS-CoV-2 diagnostics, Biosensors 13 (2) (Jan. 2023) 196, https://doi.org/10.3390/bios13020196.

[31] F.S. Possebon, et al., A fast and cheap in-house magnetic bead RNA extraction method for COVID-19 diagnosis, J. Virol. Methods 300 (Feb. 2022) 114414, https://doi.org/10.1016/j.jviromet.2021.114414 ([Not Available in CrossRef][Not Available in Internal Pubmed][Not Available in External Pubmed]).

[32] S.D. Villota, et al., Alternative RNA extraction-free techniques for the real-time RT-PCR detection of SARS-CoV-2 in nasopharyngeal swab and sputum samples, J. Virol. Methods 298 (Dec. 2021) 114302, https://doi.org/10.1016/j.jviromet.2021.114302 ([Not Available in CrossRef][Not Available in Internal Pubmed][Not Available in External Pubmed]).

[33] S.N. Rodríguez Flores, L.M. Rodríguez-Martínez, B.L. Reyes-Berrones, N.A. Fernández-Santos, E.J. Sierra-Moncada, M.A. Rodríguez-Pérez, Comparison between a standard and SalivaDirect RNA extraction protocol for molecular diagnosis of SARS-CoV-2 using nasopharyngeal swab and saliva clinical samples, Front. Bioeng. Biotechnol. 9 (Mar. 2021) 638902, https://doi.org/10.3389/fbioe.2021.638902 ([Not Available in CrossRef][Not Available in Internal Pubmed][Not Available in External Pubmed]).

[34] A.S. Fomsgaard, M.W. Rosenstierne, An alternative workflow for molecular detection of SARS-CoV-2 – escape from the NA extraction kit-shortage, Copenhagen, Denmark, March 2020, Euro Surveill. 25 (14) (Apr. 2020), https://doi.org/10.2807/1560-7917.ES.2020.25.14.2000398 ([Not Available in CrossRef][Not Available in Internal Pubmed][Not Available in External Pubmed]).

[35] Y.-I. Kim, et al., Development of severe acute respiratory syndrome coronavirus 2 (SARS-CoV-2) thermal inactivation method with preservation of diagnostic sensitivity, J. Microbiol. 58 (10) (Oct. 2020) 886–891, https://doi.org/10.1007/s12275-020-0335-6 ([Not Available in CrossRef][Not Available in Internal Pubmed][Not Available in External Pubmed]).

[36] I. Smyrlaki, et al., Massive and rapid COVID-19 testing is feasible by extraction-free SARS-CoV-2 RT-PCR, Nat. Commun. 11 (1) (Sep. 2020) 4812, https://doi.org/10.1038/s41467-020-18611-5 ([Not Available in CrossRef][Not Available in Internal Pubmed][Not Available in External Pubmed]).

[37] B. Pastorino, F. Touret, M. Gilles, X. De Lamballerie, R.N. Charrel, Heat inactivation of different types of SARS-CoV-2 samples: what protocols for biosafety, molecular detection and serological diagnostics? Viruses 12 (7) (Jul. 2020) 735, https://doi.org/10.3390/v12070735 ([Not Available in CrossRef][Not Available in Internal Pubmed][Not Available in External Pubmed]).

[38] Invitrogen, "TRIzol™ Reagent User Guide." [Online]. Available: https://tools.thermofisher.com/content/sfs/manuals/trizol_reagent.pdf.

[39] P. Chomczynski, A reagent for the single-step simultaneous isolation of RNA, DNA and proteins from cell and tissue samples, Biotechniques 15 (3) (Sep. 1993) 532–534, 536–537.

[40] K.-H. Esser, W.H. Marx, T. Lisowsky, maxXbond: first regeneration system for DNA binding silica matrices, Nat. Methods 3 (1) (Jan. 2006) i–ii, https://doi.org/10.1038/nmeth845 ([Not Available in CrossRef][Not Available in Internal Pubmed][Not Available in External Pubmed]).

[41] World Health Organization, Coronavirus Disease (COVID-19) Pandemic, Jul. 2023 [Online]. Available: https://www.who.int/emergencies/diseases/novel-coronavirus-2019?adgroupsurvey={adgroupsurvey}&gclid=CjwKCAjw-7OlBhB8EiwAnoOEk7PTqiusl76B4mZxH4YR-svONf3cB_f3UNDBnR1pjGZHlo_nkSvJSRoCSsYQAvD_BwE. (Accessed 11 July 2023).

[42] T.G.W. Graham, et al., Open-source RNA extraction and RT-qPCR methods for SARS-CoV-2 detection, PLoS One 16 (2) (Feb. 2021) e0246647, https://doi.org/10.1371/journal.pone.0246647 ([Not Available in CrossRef][Not Available in Internal Pubmed][Not Available in External Pubmed]).